

**Two electrons in one-dimensional nanorings: Exact solutions and interaction energies**

Jia-Lin Zhu\* and Zhensheng Dai

*Department of Physics, Tsinghua University, Beijing 100084, People's Republic of China*

Xiao Hu

*Computational Materials Science Center, National Institute for Materials Science, Tsukuba 305-0047, Japan*

(Received 2 December 2002; revised manuscript received 24 March 2003; published 30 July 2003)

Exact series solutions for two electrons in one-dimensional nanorings have been obtained by expanding the Coulomb potential into power series and solving the corresponding equations in different regions. Electronic structures and interaction energies of two electrons in nanorings with different sizes have been calculated. The quantum-size effect of interaction energies and energy levels and the size-dependent magnetic oscillations of two-electron spectra have been revealed.

DOI: 10.1103/PhysRevB.68.045324

PACS number(s): 73.21.-b, 73.22.-f, 75.75.+a, 71.10.Li

**I. INTRODUCTION**

Various nanometer structures are fabricated endlessly as nanostructure technology develops rapidly. They are currently under intense study because of interests in physics<sup>1-4</sup> and in technological applications. Quantum dots are one kind of useful quantum structures which can be fabricated by directly self-organized growth.<sup>5</sup> In quantum dots, multifarious quantum effects have been observed experimentally and a large number of theoretical investigations about electronic structures and related magnetic and optical properties have been performed to explain the experiments.<sup>6-12</sup> Compared with quantum dots, semiconductor quantum rings belong to another kind of topological structures in which more rich phenomena can be clearly shown. Very recently, the realization of nanoscopic semiconductor rings inside a completed field-effect transistor (FET) structure have been demonstrated by Lorke and collaborators,<sup>4,13</sup> using the self-assembly techniques. The outer radius of the rings is between 30 and 70 nm and the inter radius is about 10 nm. The nanoscopic rings are in the true quantum limit and quite different from the conventional submicron mesoscopic structures.<sup>14-23</sup>

Electron-electron interaction and correlation effects are shown to play an important role in electronic structures of both quantum dots and rings. The exact quantum levels and interaction energies of two electrons confined in quantum dots have been studied, and the size and shape effects have been clearly shown.<sup>8</sup> The energy levels and FIR spectroscopy of two-electron nanoscopic rings with a realized width have been studied.<sup>15</sup> Many body wave functions and spin order-disorder transition of realistic 2D QR's with different radii have been calculated and studied, and some of the differences and analogies between QD's and QR's have also been discussed.<sup>16</sup>

According to the realistic physical situation of two-electron rings of GaAs with larger radius ( $\sim 480$  nm) and narrower width ( $\sim 20$  nm), an adiabatic approximation allows one to decouple the radial motion from the angular motion, and then it is reasonable to use the mean Coulomb potential to describe the electron-electron interaction.<sup>17,18</sup> The mean Coulomb potential can be expanded into a power

series of the deviations ( $\gamma - \gamma_Q$ ) from the quasiequilibrium values  $\gamma_Q$  as follows:

$$\frac{e^2}{4\pi\epsilon_0\epsilon_s R \sqrt{2[1 - \cos(\gamma)]}} \approx \frac{e^2}{8\pi\epsilon_0\epsilon_s R} + \sum_{Q=-\infty}^{\infty} \frac{m_e \Omega^2 R^2}{4} \times (\gamma - \gamma_Q)^2 \Theta(\pi - |\gamma - \gamma_Q|),$$

where  $\Omega^2 = e^2 / (16\pi\epsilon_0\epsilon_s m_e R^3)$  and  $\Theta(x)$  is the Heaviside unit step function. What was mentioned above makes one arrive at analytical solutions of the wave functions and the energy spectra, and then the optical absorption and the differential cross section of resonant inelastic light scattering can be calculated and the selection rules are clearly shown.<sup>18</sup>

In the limit of a narrow-width nanoring, i.e., one-dimensional (1D) quantum ring (QR), as far as we know, the exact solutions have not been obtained, and the size effects on the interaction energies and electronic structures have not been studied. Therefore, it is interesting not only from a physical point of view but also from a mathematical point of view to find out the exact solutions of two-electron 1D QR's. In order to investigate the size and interaction effects, exact energy levels and interaction energies of two electrons in 1D QR's are obtained by expanding the Coulomb potential into power series and using the exact series solutions of the corresponding equations in different regions in this paper. Based on them, the size-dependent electronic structures and magnetic oscillations have been discussed in detail.

The remainder of this paper is organized as follows. In the next section, we introduce a model Hamiltonian and define two-electron interaction energies. In Sec. III, exact series solutions are obtained and the difference of interaction energies between singlet and triplet states is confirmed. Main results are shown and discussed in Sec. IV, followed by a summary in Sec. V.

## II. MODEL HAMILTONIAN AND INTERACTION ENERGIES

The Hamiltonian  $H$  of two interacting electrons confined in a 1D QR with a magnetic flux  $\phi$  threading through its interior is as follows:

$$H = -\frac{1}{R_0^2} \left( \frac{d}{d\varphi_1} + i\phi \right)^2 - \frac{1}{R_0^2} \left( \frac{d}{d\varphi_2} + i\phi \right)^2 + \frac{w}{R_0 |\sin[(\varphi_1 - \varphi_2)/2]|}, \quad (1)$$

where the plane polar coordinates are used.  $R_0$  is the radius of the circular ring, and the third term with  $w=1$  is the interaction between two electrons confined in the ring. Here we use the effective atomic units, in which the effective Rydberg  $\text{Ry}^* = m_e^* e^4 / 2\hbar^2 (4\pi\epsilon_0\epsilon_r)^2$ , the effective Bohr radius  $a_B^* = 4\pi\epsilon_0\epsilon_r \hbar^2 / m_e^* e^2$  and  $\phi_0 = 2\pi\hbar c / e$  are taken to be the energy, length, and magnetic flux units, respectively. For GaAs materials, for example,  $\text{Ry}^* = 5.8 \text{ meV}$ ,  $a_B^* = 10 \text{ nm}$ , and  $\phi_0$  included by a 1D ring with a radius  $a_B^*$  corresponds to the magnetic field 13.18 T.

The Hamiltonian  $H$  can be separated into center-of-mass and relative-motion terms and rewritten as

$$H = H_c + H_r, \quad (2)$$

with

$$H_c = -\frac{1}{2R_0^2} \left( \frac{d}{d\Theta} + i2\phi \right)^2 \quad (3)$$

and

$$H_r = -\frac{2}{R_0^2} \frac{d^2}{d\varphi^2} + \frac{w}{R_0 |\sin(\varphi/2)|}, \quad (4)$$

where  $\Theta = (\varphi_1 + \varphi_2)/2$  and  $\varphi = \varphi_1 - \varphi_2$ . This separability allows us to write two-particle wave functions in the form  $\Phi(\varphi_1, \varphi_2) = \Xi(\Theta)\Psi(\varphi)$ . Noting that  $\Phi(\varphi_1, \varphi_2) = \Phi(\varphi_1 + 2\pi, \varphi_2) = \Phi(\varphi_1, \varphi_2 + 2\pi) = \Phi(\varphi_1 + 2\pi, \varphi_2 + 2\pi)$  we can get the period of  $\Xi(\Theta)$  and  $\Psi(\varphi)$  to be  $2\pi$  and  $4\pi$ , respectively, and the relation as follows:

$$\Xi_M(\Theta)\Psi_{m,s}(\varphi) = \Xi_M(\Theta + \pi)\Psi_{m,s}(\varphi \pm 2\pi). \quad (5)$$

The eigenvalues and eigenfunctions of Eq. (3) are given by

$$E_c(M) = \frac{(M + 2\phi)^2}{2R_0^2} \quad (6)$$

and

$$\Xi_M(\Theta) = \frac{1}{\sqrt{2\pi}} \exp(iM\Theta) \quad (7)$$

with  $M = 0, \pm 1, \pm 2, \pm 3, \dots$ . For the spin singlet ( $s=0$ ) and triplet ( $s=1$ ) states, the eigenvalues and eigenfunctions of Eq. (4) without the interaction term ( $w=0$ ) are given by

$$E_r(m, s, w=0) = \frac{m^2}{2R_0^2} \quad (8)$$

and

$$\Psi_{m,s}(\varphi) = \begin{cases} \frac{1}{\sqrt{2\pi(1+\delta_{m,0})}} \cos(m\varphi/2) & \text{if } s=0, \\ \frac{1}{\sqrt{2\pi}} \sin(m\varphi/2) & \text{if } s=1, \end{cases} \quad (9)$$

where  $m = 0, 1, 2, 3, \dots$  for singlet states and  $m = 1, 2, 3, \dots$  for triplet states.

Based on Eqs. (5), (7), and (9), the relation  $(-1)^{M+m} = 1$  is obtained, and then  $M+m$  should be even.  $M, m$ , and  $s$  can be used to label quantum levels of two electrons with and without the interaction term in 1D QR's.  $\cos(m\varphi/2)/\sqrt{2\pi(1+\delta_{m,0})}$  and  $\sin(m\varphi/2)/\sqrt{2\pi}$  are, respectively, changed into the other even and odd functions as the interaction term is included.

The eigenenergies  $E_0(M, m, s)$  of  $H$  with  $w=0$  are

$$E_0(M, m, s) = E_c(M) + E_r(m, s, w=0) = \frac{(M + 2\phi)^2 + m^2}{2R_0^2}, \quad (10)$$

while the eigenenergies  $E(M, m, s)$  of  $H$  with  $w=1$  are given by

$$E(M, m, s) = E_c(M) + E_r(m, s) = \frac{(M + 2\phi)^2}{2R_0^2} + E_r(m, s), \quad (11)$$

where the eigenvalues  $E_r(m, s)$  and the corresponding eigenfunctions of Eq. (4) can be obtained by expanding the potential term into power series and using the exact series solutions with proper boundary conditions in the next section. For the sake of convenience, we define the electron-electron interaction energies  $E_{in}(M, m, s)$  as the difference between  $E(M, m, s)$  and  $E_0(M, m, s)$ , i.e.,

$$E_{in}(M, m, s) = E(M, m, s) - E_0(M, m, s) = E_r(m, s) - \frac{m^2}{2R_0^2} \quad (12)$$

which are independent on  $M$ .

## III. EXACT SOLUTIONS

In order to obtain  $E_r(m, s)$ , we should solve the Schrödinger-like equation

$$H_r \Psi_{m,s}(\varphi) = E_r(m, s) \Psi_{m,s}(\varphi) \quad (13)$$

which can be simplified as follows:

$$\frac{d^2 \Psi(\varphi)}{d\varphi^2} - V(\varphi) \Psi(\varphi) = 0 \quad (14)$$

with

$$V(\varphi) = \frac{R_0}{2|\sin(\varphi/2)|} - \frac{R_0^2}{2} E_r(m,s). \quad (15)$$

It is only needed to solve the equation in the region of  $[0, 2\pi)$ , and  $\Psi_{m,s}(\varphi)$  in other regions can be obtained by using Eqs. (5) and (7), i.e.,

$$\Psi_{m,s}(\varphi) = (-1)^M \Psi_{m,s}(\varphi \pm 2\pi). \quad (16)$$

It should be noted that zero and  $2\pi$  are regular singular points of  $V(\varphi)$ . It can be, respectively, expanded into Laurent and Taylor series around the regular singular point  $\varphi_r = 0$  and  $2\pi$  and at the normal points  $\varphi_r \in (0, 2\pi)$  up to the  $K$ th order in the form

$$V(\varphi) = \begin{cases} \sum_{i=-1}^K u_i (\varphi - \varphi_r)^i & \text{for } \varphi_r = 0 \text{ and } 2\pi, \\ \sum_{i=0}^K v_i (\varphi - \varphi_r)^i & \text{for } \varphi_r \in (0, 2\pi). \end{cases} \quad (17)$$

For the sake of convenience,  $R$  points including two regular singular points are taken. The regular singular points correspond to  $r=1$  and  $R$ , and  $\varphi_r$  with  $r=2, 3, \dots$ , and  $R-1$  are normal points. For example, the Laurent series around zero and the Taylor series at  $\pi$  are, respectively, as follows:

$$V(\varphi) = R_0 \varphi^{-1} - \frac{R_0^2}{2} E_r(m,s) + \frac{1}{24} R_0 \varphi + \frac{7}{5760} R_0 \varphi^3 + \frac{31}{967680} R_0 \varphi^5 + \frac{127}{154828800} R_0 \varphi^7 + \dots \quad (18)$$

and

$$V(\varphi) = \frac{1}{2} R_0 - \frac{R_0^2}{2} E_r(m,s) + \frac{1}{16} R_0 (\varphi - \pi)^2 + \frac{5}{768} R_0 (\varphi - \pi)^4 + \frac{61}{92160} R_0 (\varphi - \pi)^6 + \dots \quad (19)$$

It should be pointed out that the maximal error of the series expansions up to the  $K$ th order can be extremely small

$$Y_l = \begin{cases} \sum_{i=l-1}^K \frac{(i+1)!}{l!(i-l+1)!} u_i (\varphi_t - \varphi_r)^{i-l+1} & \text{for } \varphi_r = 0 \text{ or } 2\pi, \\ \sum_{i=\max(0, l-1)}^K \frac{(i+1)!}{l!(i-l+1)!} v_i (\varphi_t - \varphi_r)^{i-l+1} & \text{for } \varphi_r \in (0, 2\pi). \end{cases} \quad (24)$$

The recurrence relations of  $d_n^t$  are similar to those of  $c_n^t$ .

Using the matching conditions between the exact series solutions at the proper points  $\varphi_t^* \in [\varphi_t, \varphi_{t+1}]$ , in general,  $\varphi_t^* = (\varphi_t + \varphi_{t+1})/2$ , and the  $2 \times 2$  transfer matrices, we can

as long as a proper number  $R$  and the corresponding positions of series expansion points  $(\varphi_1, \varphi_2, \dots, \varphi_R)$  are chosen. For instance, the maximal error of  $V(\varphi)/R_0$  in the whole region  $[0, 2\pi)$  is less than  $1.0E-14$  when  $K$  and  $R$  are equal to 23 and 5, respectively. It can be seen that a higher accuracy required in numerical calculations is easily reached by increasing the  $R$  or the  $K$  without more computation time consumption.

Once the series expansion forms of  $V(\varphi)$  in different regions are obtained, the exact series solutions can be found.<sup>8</sup> In the region  $\varphi \rightarrow 0$  or  $\varphi \rightarrow 2\pi$  we have an exact series solution, which has a finite value at  $\varphi_r = 0$  or  $2\pi$  as follows:

$$\Psi(\varphi) = A_r (\varphi - \varphi_r) \sum_{n=0}^{\infty} a_n^r (\varphi - \varphi_r)^n, \quad (20)$$

where  $A_r$  is a constant and  $a_0^r$  is equal to 1. Noting that  $a_n^r$  is equal to zero as  $n$  is equal to a negative integer, the other  $a_n^r$  can be determined by the following recurrence relation:

$$a_n^r = \frac{1}{n(n+1)} \sum_{i=-1}^{\min(K, n-2)} u_i a_{n-i-2}^r. \quad (21)$$

In order to match the solutions of Eq. (20) with  $\varphi_r = 0$  and  $\varphi_r = 2\pi$ , we give  $T$  solutions around  $\varphi_1, \varphi_2, \dots, \varphi_t, \dots$ , and  $\varphi_T$ , which are the proper points for solving Eq. (14) exactly. The solution of uniformly convergent Taylor series around  $\varphi_t (t=1, 2, \dots, T)$  is written as follows:

$$\Psi(\varphi) = C_t \sum_{n=0}^{\infty} c_n^t (\varphi - \varphi_t)^n + D_t \sum_{n=0}^{\infty} d_n^t (\varphi - \varphi_t)^n, \quad (22)$$

where  $C_t$  and  $D_t$  are constants,  $c_0^t$  and  $d_0^t$  are equal to 1, and  $c_1^t$  and  $d_1^t$  are equal to 0. The  $c_n^t$  and  $d_n^t$  can be determined by the recurrence relations

$$c_n^t = \frac{1}{n(n-1)(\varphi_t - \varphi_r)} \left\{ -(n-1)(n-2)c_{n-1}^t + \sum_{l=0}^{\min(K+1, n-2)} Y_l c_{n-l-2}^t \right\}, \quad (23)$$

where  $Y_l$  are related to the expanding point  $\varphi_r$  and the corresponding coefficients in Eq. (17) as follows:

easily deduce the equation for eigenenergies of Eq. (13). Both eigenenergies  $E_r(j)$  and wave functions  $\Psi_j(\varphi)$  in  $[0, 2\pi)$  with  $j(j=0, 1, 2, 3, \dots)$  nodes are obtained numerically. It should be pointed out that  $T \geq R-2$  and, in general,

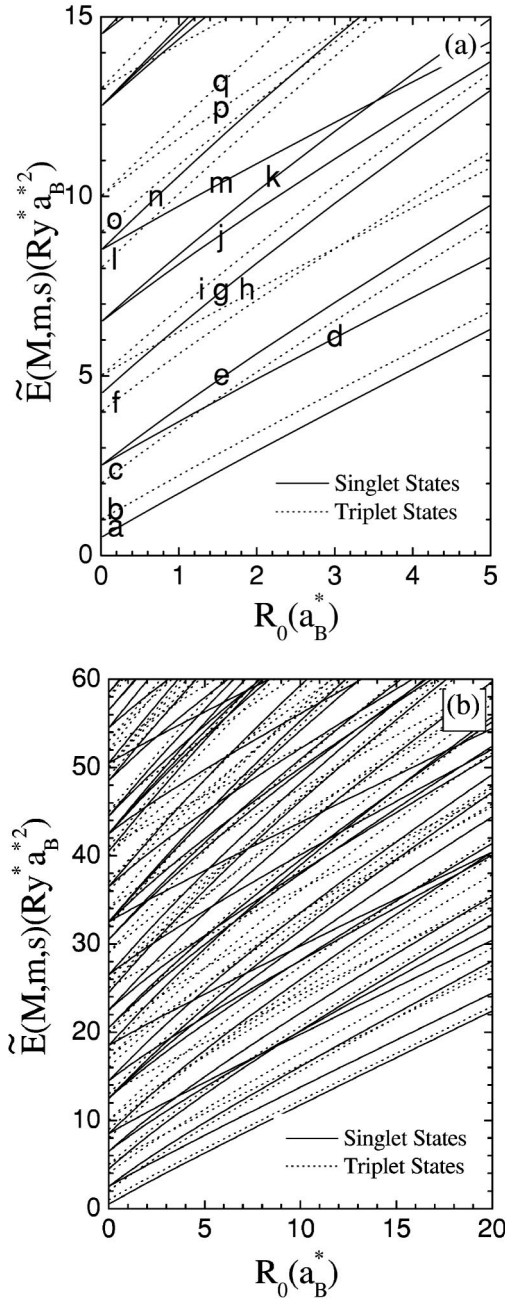


FIG. 1. Normalized total energies  $\tilde{E}(M, m, s)$  of two electrons versus  $R_0$ . The quantum numbers of  $a, b, c, \dots, p, q$  states are listed in Table I.

$T$  is much larger than  $R$  and that in numerical calculations the larger  $T$  is taken, the less terms of the exact series solutions are required.

Because  $V(\varphi)$  is symmetrical about  $\varphi = \pi$ , we have  $\Psi_j(\varphi + \pi) = (-1)^j \Psi_j(-\varphi + \pi)$ , i.e.,  $\Psi_j(\varphi) = (-1)^j \Psi_j(2\pi - \varphi)$ . Then we can get  $\Psi_j(\varphi) = (-1)^{M+j} \Psi_j(-\varphi)$  with use of Eq. (16), and we have  $M + j$  to be even and odd for singlet and triplet states, respectively. Noting that  $E_r(m, 0) = E_r(m + 1, 1)$  and that  $E_{\text{in}}(M, m, 0) = E_r(m, 0) - m^2/2R_0^2$  and  $E_{\text{in}}(M \pm 1, m + 1, 1) = E_r(m + 1, 1) - (m + 1)^2/2R_0^2$ , we have

TABLE I. Exact energy levels  $\tilde{E}(M, m, s)$  of two electrons in 1D QR's with different  $R_0$ . The level sequences are in order of increasing magnitude. For the sake of convenience, the short notation about quantum numbers and spin, i.e.,  $a, b, c$ , etc., in the order of increasing energy value under very strong confined condition of  $R_0 \rightarrow 0$ , is used to show the change of the level order.

$R_0(a_B^*)$		1		4		20	
$a$ :	$\tilde{E}(0,0,0)$	(a)	1.73174	(a)	5.18474	(a)	22.40328
$b$ :	$\tilde{E}(\pm 1,1,1)$	(b)	2.23174	(b)	5.68474	(b)	22.90328
$c$ :	$\tilde{E}(0,2,1)$	(c)	3.61722	(d)	7.18474	(d)	24.40328
$d$ :	$\tilde{E}(\pm 2,0,0)$	(d)	3.73174	(c)	7.91615	(h)	26.90328
$e$ :	$\tilde{E}(\pm 1,1,0)$	(e)	4.11722	(e)	8.41615	(c)	27.54199
$f$ :	$\tilde{E}(\pm 2,2,1)$	(f)	5.61722	(h)	9.68474	(e)	28.04199
$g$ :	$\tilde{E}(0,2,0)$	(h)	6.23174	(f)	9.91615	(f)	29.54199
$h$ :	$\tilde{E}(\pm 3,1,1)$	(g)	6.38133	(g)	11.40424	(m)	30.40328
$i$ :	$\tilde{E}(\pm 1,3,1)$	(i)	6.88133	(i)	11.90424	(j)	32.04199
$j$ :	$\tilde{E}(\pm 3,1,0)$	(j)	8.11722	(j)	12.41615	(g)	33.36149
$k$ :	$\tilde{E}(\pm 2,2,0)$	(k)	8.38133	(m)	13.18474	(i)	33.86149
$l$ :	$\tilde{E}(0,4,1)$	(m)	9.73174	(k)	13.40424	(k)	35.36149
$m$ :	$\tilde{E}(\pm 4,0,0)$	(l)	10.07614	(l)	15.70729	(p)	35.54199
$n$ :	$\tilde{E}(\pm 1,3,0)$	(n)	10.57614	(o)	15.90424	(o)	37.86149
$o$ :	$\tilde{E}(\pm 3,3,1)$	(o)	10.88133	(p)	15.91615	(l)	39.89374
$p$ :	$\tilde{E}(\pm 4,2,1)$	(p)	11.61722	(n)	16.20729	(n)	40.39374
$q$ :	$\tilde{E}(\pm 2,4,1)$	(q)	12.07614	(q)	17.70729	(q)	41.89374

$$E_{\text{in}}(M, m, 0) - E_{\text{in}}(M \pm 1, m + 1, 1) = \frac{m + 1/2}{R_0^2}. \quad (25)$$

#### IV. RESULTS AND DISCUSSION

We have performed numerical calculations for energy levels  $E(M, m, s)$  of two electrons in 1D QR's with different  $R_0$ . For the sake of convenience, the normalized energy levels  $\tilde{E}(M, m, s)$  which are  $E(M, m, s)$  multiplied by  $R_0^2$  are used. As  $R_0$  changes from  $0.1a_B^*$  to  $20a_B^*$ ,  $\tilde{E}(M, m, s)$  increase and the level order varies greatly as shown in Fig. 1 and Table I. In Fig. 1(a), the lowest intersection of two levels  $\tilde{E}(0, 2, 1)$  and  $\tilde{E}(2, 0, 0)$ , i.e.,  $\tilde{E}(0, 2, 1) = \tilde{E}(2, 0, 0) = 4.1\text{Ry}^* a_B^{*2}$  with different spin can be found at  $R_0 = 1.3a_B^*$ , and there are much more intersections of higher levels with same or different spin in Fig. 1(b). Those intersections show the quantum size effect induced by the electron-electron interactions.

For a better understanding of the quantum size effect, the electron-electron interaction energies  $E_{\text{in}}(M, m, s)$  defined by Eq. (12) are studied. For the sake of clearness, the normalized interaction energies  $\tilde{E}_{\text{in}}(M, m, s) = E_{\text{in}}(M, m, s)R_0^2$  are introduced. As mentioned above  $\tilde{E}_{\text{in}}(M, m, s)$  in which  $M + m$  must be even are independent of  $M$ . As shown in Fig. 2 and Table II,  $\tilde{E}_{\text{in}}(M, m, 0)$  and  $\tilde{E}_{\text{in}}(M \pm 1, m + 1, 1)$  approach  $m + \frac{1}{2}$  and zero as  $R_0$  becomes small, and it is in agreement

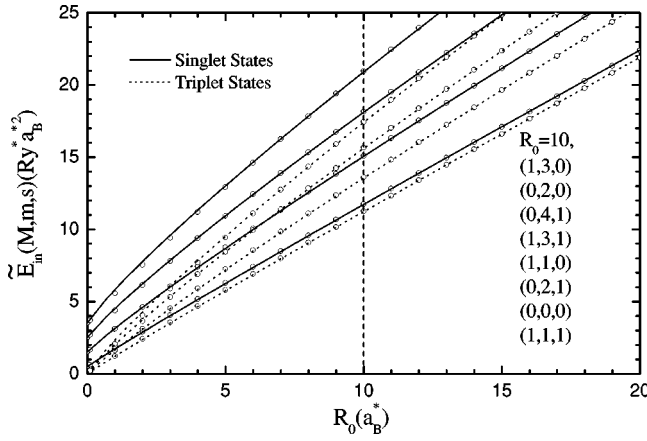


FIG. 2.  $\tilde{E}_{\text{in}}(M, m, s)$  versus  $R_0$ . The part of solid circles is interaction energies shown in Table II, and the lines are obtained by nonlinear fitting with parameters in Table III. The order of  $\tilde{E}_{\text{in}}(M, m, s)$  at  $R_0 = 10a_B^*$  is noted in the figure.

with Eq. (25). All values of  $\tilde{E}_{\text{in}}(M, m, 0)$  are larger than those of  $\tilde{E}_{\text{in}}(M', m', 1)$  at  $R_0 = 0.1a_B^*$ , and the situation is changed as  $R_0$  increases.  $\tilde{E}_{\text{in}}(M \pm 1, m + 1, s)$  are larger than  $\tilde{E}_{\text{in}}(M, m, s)$  and their differences are much larger for large  $R_0$ . It is worthwhile to point out that the crossover between  $\tilde{E}_{\text{in}}(M, m, 0)$  and  $\tilde{E}_{\text{in}}(M', m', 1)$  can appear as  $R_0$  changes from 0 to a finite value. The behavior of the interaction energies of 1D QR's is quite different from that of 2D QD's with parabolic potentials,<sup>8</sup> in which the normalized interaction energies decrease with increasing the relative angular momentum. What mentioned above can be understood from the

TABLE II. Exact interaction energies  $\tilde{E}_{\text{in}}(M, m, s)$  of two electrons in 1DQR's with different  $R_0$ .

$R_0(a_B^*)$	0.1	1.0	10
$\tilde{E}_{\text{in}}(0,0,0)$	0.626809508	1.731743163	11.75359702
$\tilde{E}_{\text{in}}(1,1,0)$	1.668829593	3.117217611	15.10196848
$\tilde{E}_{\text{in}}(0,2,0)$	2.694483873	4.381327404	18.15519236
$\tilde{E}_{\text{in}}(1,3,0)$	3.712839318	5.576142929	20.95569979
$\tilde{E}_{\text{in}}(0,4,0)$	4.727105767	6.728294117	23.54045018
$\tilde{E}_{\text{in}}(1,5,0)$	5.738766402	7.852265289	25.94128634
$\tilde{E}_{\text{in}}(0,6,0)$	6.748623604	8.956505108	28.18533850
$\tilde{E}_{\text{in}}(1,7,0)$	7.757159619	10.04627088	30.29561158
$\tilde{E}_{\text{in}}(1,1,1)$	0.126809508	1.231743163	11.25359702
$\tilde{E}_{\text{in}}(0,2,1)$	0.168829593	1.617217611	13.60196848
$\tilde{E}_{\text{in}}(1,3,1)$	0.194483873	1.881327404	15.65519236
$\tilde{E}_{\text{in}}(0,4,1)$	0.212839318	2.076142929	17.45569979
$\tilde{E}_{\text{in}}(1,5,1)$	0.227105767	2.228294117	19.04045018
$\tilde{E}_{\text{in}}(0,6,1)$	0.238766402	2.352265289	20.44128634
$\tilde{E}_{\text{in}}(1,7,1)$	0.248623604	2.456505108	21.68533850
$\tilde{E}_{\text{in}}(0,8,1)$	0.257159619	2.546270881	22.79561158

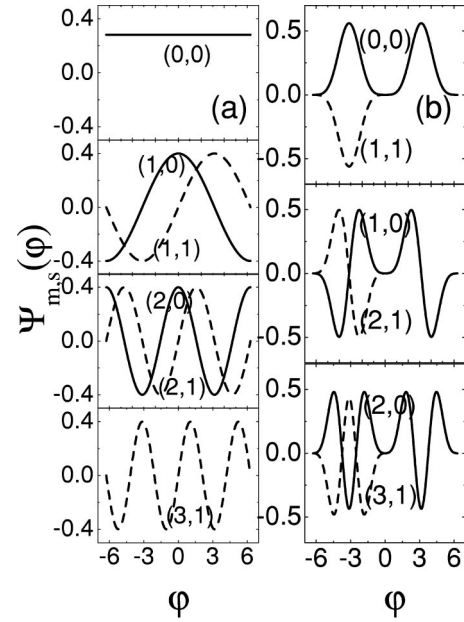


FIG. 3. Relative-motion wave functions  $\Psi_{m,s}(\varphi)$  of two electrons versus  $\varphi$  in a ring of  $R_0 = 20a_B^*$  (a) without and (b) with the Coulomb interaction term.

distribution of the relative-motion wave functions  $\Psi_{m,s}(\varphi)$  and their variation induced by the singularity of the Coulomb potential.

In Fig. 3, the  $\Psi_{m,s}(\varphi)$  of singlet and triplet states with and without the Coulomb interaction are plotted. From the difference between wave functions with and without the

TABLE III. Nonlinear fitting parameters of  $\tilde{E}_{\text{in}}(M, m, s)$  with use of the form  $\tilde{E}_{\text{in}}(M, m, s, R_0) = A_{m,s} + B_{m,s}R_0^{C_{m,s}}$ .

Singlet states	$A_{m,s}$	$B_{m,s}$	$C_{m,s}$
$\tilde{E}_{\text{in}}(0,0,0)$	0.5	1.21914	0.96453
$\tilde{E}_{\text{in}}(1,1,0)$	1.5	1.64921	0.91509
$\tilde{E}_{\text{in}}(0,2,0)$	2.5	2.02440	0.88713
$\tilde{E}_{\text{in}}(1,3,0)$	3.5	2.34133	0.87145
$\tilde{E}_{\text{in}}(0,4,0)$	4.5	2.60500	0.86319
$\tilde{E}_{\text{in}}(1,5,0)$	5.5	2.82287	0.85956
$\tilde{E}_{\text{in}}(0,6,0)$	6.5	3.00247	0.85891
$\tilde{E}_{\text{in}}(1,7,0)$	7.5	3.15052	0.86018
Triplet States	$A_{m,s}$	$B_{m,s}$	$C_{m,s}$
$\tilde{E}_{\text{in}}(1,1,1)$	0.0	1.21914	0.96453
$\tilde{E}_{\text{in}}(0,2,1)$	0.0	1.64921	0.91509
$\tilde{E}_{\text{in}}(1,3,1)$	0.0	2.02440	0.88713
$\tilde{E}_{\text{in}}(0,4,1)$	0.0	2.34133	0.87145
$\tilde{E}_{\text{in}}(1,5,1)$	0.0	2.60500	0.86319
$\tilde{E}_{\text{in}}(0,6,1)$	0.0	2.82287	0.85956
$\tilde{E}_{\text{in}}(1,7,1)$	0.0	3.00247	0.85891
$\tilde{E}_{\text{in}}(0,8,1)$	0.0	3.15052	0.86018

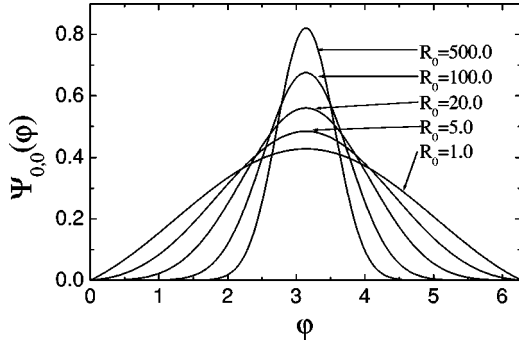


FIG. 4.  $\Psi_{0,0}(\varphi)$  versus  $\varphi \in [0, 2\pi)$  for  $R_0 = 1.0, 5.0, 20.0, 100.0, 500.0 a_B^*$ .

Coulomb interaction, it is easy to evaluate the magnitude of interaction energies  $E_{in}$ . For example, there are two more nodes in  $\Psi_{0,0}(\varphi)$  with the Coulomb interaction than in that without the Coulomb interaction. The number of nodes in  $\Psi_{1,1}(\varphi)$  with the Coulomb interaction is equal to that without the Coulomb interaction, and then  $\tilde{E}_{in}(M, 0, 0) > \tilde{E}_{in}(M$

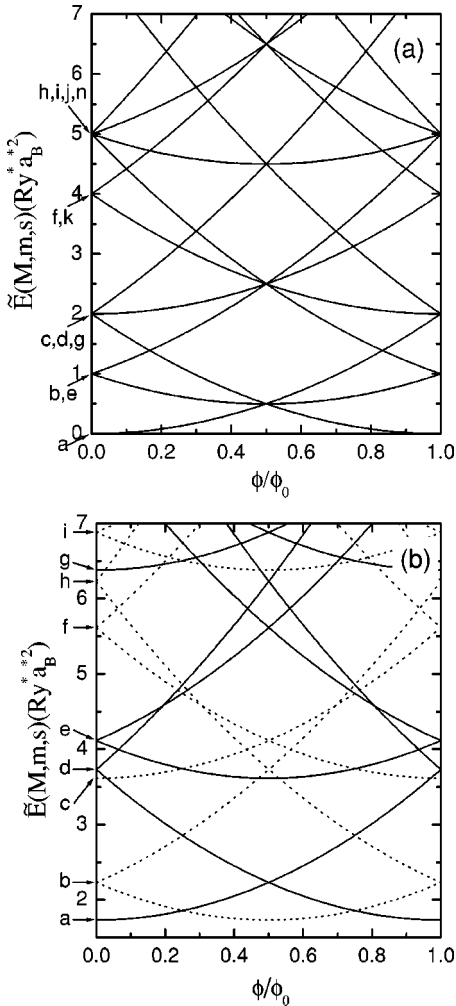


FIG. 5.  $\tilde{E}(M, m, s, R_0, \phi)$  versus  $\phi$  for (a)  $w=0$  and any  $R_0$  and (b)  $w=1$  and  $R_0 = 1a_B^*$ . The quantum numbers of  $a, b, c, \dots$ , states are listed in Table I.

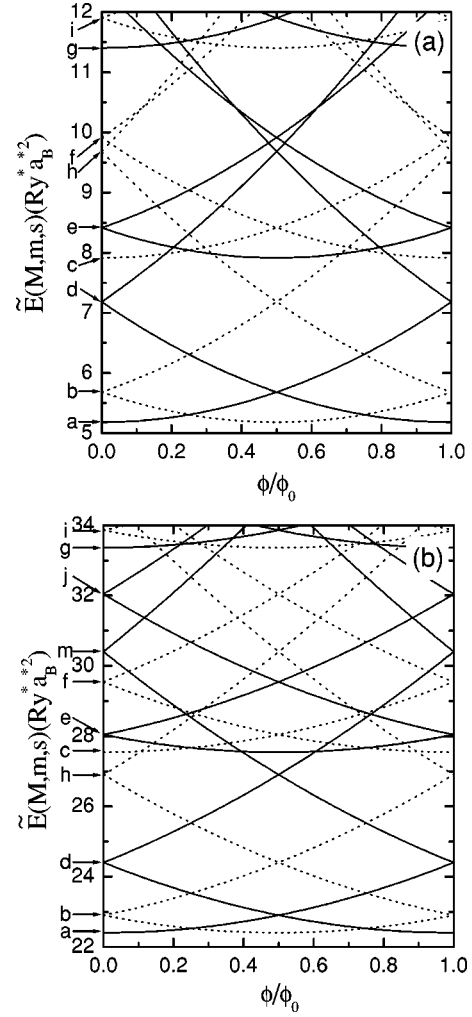


FIG. 6.  $\tilde{E}(M, m, s, R_0, \phi)$  versus  $\phi$  for (a)  $w=1$  and  $R_0 = 4a_B^*$  and (b)  $w=1$  and  $R_0 = 20a_B^*$ . The quantum numbers of  $a, b, c, \dots$ , states are listed in Table I.

$\pm 1, 1, 1$ ). In Fig. 4,  $\Psi_{0,0}(\varphi)$  with different  $R_0$  has been plotted, and it is localized at  $\varphi = \pi$  gradually as  $R_0$  increases from  $1a_B^*$  to  $500a_B^*$ . The situation of  $\Psi_{m,s}(\varphi)$  is similar, so that behavior of two electrons in large rings is more similar to a Wigner molecule<sup>19,20</sup> than that in small ones, and then  $\tilde{E}_{in}(E_{in})(M, m, 1)$  is not proportional to  $R_0(1/R_0)$  exactly, however, it would be proportional to  $R_0^{1-\delta}(R_0^{-1-\delta})$  with  $\delta > 0$  which is dependent on  $m$  and  $s$ . Furthermore,  $\tilde{E}_{in}(M, m, 0) = \tilde{E}_{in}(M \pm 1, m + 1, 1) + m + \frac{1}{2}$  as mentioned in Eq. (25).

According to the characteristics of  $\tilde{E}_{in}(M, m, s)$  and  $\Psi_{M,m,s}(\varphi)$ , we have found a formula

$$\tilde{E}_{in}(M, m, s, R_0) = A_{m,s} + B_{m,s} R_0^{C_{m,s}}, \quad (26)$$

where  $A_{m,0} = m + 1/2$  and  $A_{m,1} = 0$ .  $B_{m,0} = B_{m+1,1}$  and  $C_{m,0} = C_{m+1,1}$ , which can be obtained by a nonlinear curve fitting with use of exact calculated results. The fitting results are listed in Table III. There are several points which should be noted. With increasing  $m$ , all  $B_{m,s}$  and  $C_{m,s}$  increase and

decrease, respectively, and  $C_{m,s}$  is always less than 1, i.e.,  $C_{m,s} = 1 - \delta_{m,s}$ , with  $\delta_{m,s} > 0$ . It is consistent with what is mentioned above. Furthermore, we can give the energies of two electrons in nanorings as follows:

$$\tilde{E}(M, m, s, R_0, \phi) = \frac{(M + 2\phi)^2 + m^2}{2} + A_{m,s} + B_{m,s} R_0^{C_{m,s}}. \quad (27)$$

By using Eq. (27), the electronic structures and related properties can be easily shown. The energy levels of two electrons in a 1D QR as a function of magnetic flux  $\phi$  have been plotted in Figs. 5 and 6. As shown in Eq. (11) or (27),  $\phi$  is for nothing in  $E_r(m, s)$  so that the period of the energy oscillations is 0.5. For instance,  $\tilde{E}(0, 0, 0)(\phi = 0)$  is equal to  $\tilde{E}(-1, 1, 1)(\phi = 0.5)$  and  $\tilde{E}(-2, 0, 0)(\phi = 1.0)$  and the spin of two electrons is oscillating too. The oscillations of  $\tilde{E}(0, 2, 1)$  and  $\tilde{E}(-1, 1, 0)$  is similar to those of  $\tilde{E}(0, 0, 0)$  and  $\tilde{E}(-1, 1, 1)$ . However, for a 1D QR with different  $R_0$ , the level order is changed by adding interaction energies as shown in Figs. 5 and 6. As  $R_0$  changes, the oscillation pictures, i.e., so called magnetic fingerprints, are changed. It means that the Coulomb interaction of two electrons in 1D QR's causes quantum size effects and makes magnetic fingerprints.

## V. SUMMARY

In this paper, an effective method, which can solve Schrödinger-like equations related to different kinds of potentials even with singular points and allow to easily reach high accuracy, is set up by expanding potentials into power series and solving the equations to get exact series solutions in different regions. Using the method, we have obtained the

exact solutions of two electrons in 1D QR's. It is worthwhile to point out that the periodic boundary conditions are important for determining the exact solutions of singlet and triplet states. In the case, without the interaction term, i.e.,  $w = 0$ , the analytical solutions are shown in Eqs. (6)–(9) and  $M + m$  should be even. In the case of  $w = 1$ , however, the condition  $\Psi_j(\varphi) = (-1)^{M+j} \Psi_j(-\varphi)$  should be used to determine the singlet and triplet states and their difference of interaction energies.

The electron-electron interaction plays a significant role in the order of quantum levels and size-dependent phenomena. The interaction energies  $\tilde{E}_{\text{in}}(M, m, s)$  in which  $M + m$  must be even are independent of  $M$  and  $\tilde{E}_{\text{in}}(M, m, 0)$  is always larger than  $\tilde{E}_{\text{in}}(M', m + 1, 1)$ . Additionally,  $\tilde{E}_{\text{in}}(M, m, s)$  increase with  $m$ , while those of 2D QD's decrease with increasing the relative angular moment.<sup>8</sup>

Noting the singularity of the Coulomb potential and the variation of wave functions with  $R_0$  in 1D QR's, the  $R_0$  dependence of interaction energies has been found by the nonlinear fitting method with use of the exact calculated results. Based on the form of Eq. (27), the  $R_0$ -dependent  $\tilde{E}(M, m, s)$  and their magnetic oscillations are clearly shown. It may be useful for the further theoretical and experimental studies of narrow quantum rings.

## ACKNOWLEDGMENT

One of the authors (J.-L.Z.) expresses his sincere thanks to Computational Materials Science Center, NIMS, and to all of the members in the research group for their kind hospitality during his stay in Tsukuba. Financial support from NSF-China (Grant No. 90101003) and China's "863" program are gratefully acknowledged.

\*Email address: zjl-dmp@tsinghua.edu.cn

<sup>1</sup>L.P. Kouwenhoven, T.H. Oosterkamp, M.W.S. Danoesastro, M. Eto, D.G. Austing, T. Honda, and S. Tarucha, *Science* **278**, 1788 (1997).

<sup>2</sup>A. Fuhrer, S. Lüscher, T. Ihn, T. Helnzel, K. Ensslin, W. Wegschelder, and M. Bichler, *Nature (London)* **413**, 822 (2001).

<sup>3</sup>P.A. Maksym, H. Imamura, G.P. Mallon, and H. Aoki, *J. Phys.: Condens. Matter* **12**, R299 (2000).

<sup>4</sup>R.J. Warburton, C. Schäfflein, D. Haft, F. Blckel, A. Lorke, K. Karal, J.M. Garcia, W. Schoenfeld, and P.M. Petroff, *Nature (London)* **405**, 926 (2000).

<sup>5</sup>J.M. Marzin, J.M. Gérard, A. Izraël, D. Barrier, and G. Bastard, *Phys. Rev. Lett.* **73**, 716 (1994).

<sup>6</sup>P.A. Maksym and T. Chakraborty, *Phys. Rev. Lett.* **65**, 108 (1990).

<sup>7</sup>S. Tarucha, D.G. Austion, T. Honda, R.J. van der Hage, and L.P. Kouwenhoven, *Phys. Rev. Lett.* **77**, 3613 (1996).

<sup>8</sup>J.L. Zhu, Z.Q. Li, J.Z. Yu, K. Ohno, and Y. Kawazoe, *Phys. Rev. B* **55**, 15 819 (1997).

<sup>9</sup>K. Kawamura and M. Eto, *Jpn. J. Appl. Phys.* **38**, 366 (1999).

<sup>10</sup>C.E. Creffield, W. Häusler, J.H. Jefferson, and S. Sarkar, *Phys.*

*Rev. B* **59**, 10 719 (1999).

<sup>11</sup>G. Cantele, D. Ninno, and G. Iadonisi, *Phys. Rev. B* **64**, 125325 (2001).

<sup>12</sup>T. Fujisawa, D.G. Austion, Y. Tokura, Y. Hirayama, and S. Tarucha, *Nature (London)* **419**, 278 (2002).

<sup>13</sup>A. Lorke, R.J. Luyken, A.O. Govorov, J.P. Kotthaus, J.M. Garcia, and P.M. Petroff, *Phys. Rev. Lett.* **84**, 2223 (2000).

<sup>14</sup>T. Chakraborty and P. Pietiläinen, *Phys. Rev. B* **50**, 8460 (1994).

<sup>15</sup>H. Hu, J.L. Zhu, and J.J. Xiong, *Phys. Rev. B* **62**, 16 777 (2000).

<sup>16</sup>P. Borrmann and J. Harting, *Phys. Rev. Lett.* **86**, 3120 (2001).

<sup>17</sup>L. Wendler and V.M. Fomin, *Phys. Rev. B* **51**, 17 814 (1995).

<sup>18</sup>L. Wendler, V.M. Fomin, A.V. Chaplik, and A.O. Govorov, *Phys. Rev. B* **54**, 4794 (1996).

<sup>19</sup>A. Puente and L. Serra, *Phys. Rev. B* **63**, 125334 (2001).

<sup>20</sup>M. Koskinen, M. Manninen, B. Mottelson, and S.M. Reimann, *Phys. Rev. B* **63**, 205323 (2001).

<sup>21</sup>A. Emperador, M. Pi, M. Barranco, and A. Lorke, *Phys. Rev. B* **62**, 4573 (2000).

<sup>22</sup>A. Emperador, M. Pi, M. Barranco, and E. Lipparini, *Phys. Rev. B* **64**, 155304 (2001).

<sup>23</sup>J.B. Xia and S.S. Li, *Phys. Rev. B* **66**, 035311 (2002).